Intermetallic Formation in Sn3Ag0.5Cu and Sn3Ag0.5Cu0.06Ni0.01Ge Solder BGA Packages with Immersion Ag Surface Finish

TUNG-HAN CHUANG,[1,2] SHIU-FANG YEN,[1] and HUI-MIN WU[1]

1.—Institute of Materials Science and Engineering, National Taiwan University, Taipei 106, Taiwan. 2.—E-mail: tunghan@ntu.edu.tw

The intermetallic compounds formed in Sn3Ag0.5Cu and Sn3Ag0.5Cu0.06Ni0.01Ge solder BGA packages with Ag/Cu pads are investigated. After reflow, scallop-shaped η-Cu_6Sn_5 and continuous planar η-$(Cu_{0.9}Ni_{0.1})_6Sn_5$ intermetallics appear at the interfaces of the Sn3Ag0.5Cu and Sn3Ag0.5Cu0.06Ni0.01Ge solder joints, respectively. In the case of the Sn3Ag0.5Cu specimens, an additional ε-Cu_3Sn intermetallic layer is formed at the interface between the η-Cu_6Sn_5 and Cu pads after aging at 150°C, while the same type of intermetallic formation is inhibited in the Sn3Ag0.5Cu0.06Ni0.01Ge packages. In addition, the coarsening of Ag_3Sn precipitates also abates in the solder matrix of the Sn3Ag0.5Cu0.06Ni0.01Ge packages, which results in a slightly higher ball shear strength for the specimens.

Key words: Sn3Ag0.5Cu, Sn3Ag0.5Cu0.06Ni0.01Ge, immersion Ag surface finish, intermetallic compounds

INTRODUCTION

Among the types of lead-free solders, the eutectic Sn-Ag-Cu alloy has drawn special attention due to its features of superior strength, ductility, and resistance to creep and fatigue.[1] Efforts have already been made to add a fourth element into the ternary Sn-Ag-Cu solder so that this alloy system can truly replace traditional Sn-Pb solders. A number of studies have found that the excessive intermetallic growth at the interfaces between Sn-Ag-Cu solder and Cu substrate could be inhibited during the aging[2,3] and reflow processes[4] with the addition of a small amount of Sb into the solder alloys. Anderson et al. reported that co-enhanced Sn-Ag-Cu solder joints exhibited the least sensitivity of shear strength to cooling rate due to the microstructure refinement in the solder matrix and at the solder/Cu substrate interface.[5] The effects of the addition of Bi on microstructure refinement and interfacial intermetallics inhibition in Sn-Ag-Cu solder joints have also been ascertained by Zhao et al.[6] By further adding a trace amount of Ge into the bi-enhanced Sn-Ag-Cu solders, Habu et al. demonstrated various improved mechanical properties, such as strength, thermal fatigue life, creep rupture time, and mechanical shock resistance.[7] By adding 0.25 wt% Ce into a Sn3.8Ag0.5Cu solder, Chen et al. attained a 7-fold increase of its creep rupture life.[8] In another recent study on the constitutive relations of creep behaviors for such rare-earth (RE) modified Sn-Ag-Cu solders, Chen et al. indicated that the creep stress exponents for Sn3.8Ag0.7Cu0.1RE solder joints were 8.2 and 14.6 at low and high stresses, respectively, both of which were higher than those for the case of undoped Sn3.8Ag0.7Cu.[9]

Sn3Ag0.5Cu0.06Ni0.01Ge is an innovative Pb-free solder developed by Japan's Fuzi Electrical Co (Osaka, Japan). Ni was added into this alloy to improve its thermal fatigue resistance, while the addition of Ge increases its wettability and decreases dross formation.[10] The effects of Ni on the intermetallic formation of Sn-Ag-Cu solders have also been studied by Chuang and Lin by dipping the Cu plates into liquid Sn-3.5Ag-0.7Cu and Sn-3.5Ag-0.5Cu-0.07Ni-0.01Ge solders at 250°C for 15 sec. They reported that the Ni-containing Sn-Ag-Cu solder possessed much thicker interfacial intermetallic com-

(Received May 24, 2005; accepted October 19, 2005)

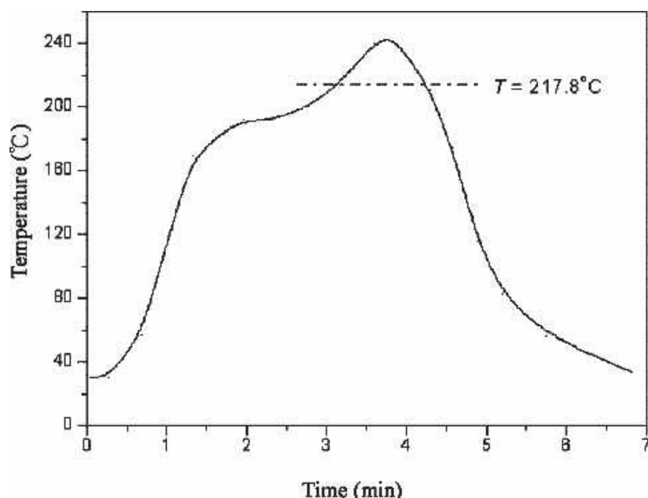

Fig. 1. Temperature profile for the reflow process of the Sn-Ag-Cu solder BGA packages with the immersion Ag surface finish described in this study.

pounds in comparison with the undoped Sn-3.5Ag-0.7Cu alloy.[11–13] However, after further aging from 105 to 150°C, the Sn-3.5Ag-0.7Cu solder exhibited a much higher intermetallic growth rate than the Sn-3.5Ag-0.5Cu-0.07Ni-0.01Ge solder.[11–13] In this present study, the influences of Ni microalloying in Sn-Ag-Cu solders on intermetallic growth are reconfirmed through the reflow and aging of Sn-3Ag-0.5Cu and Sn-3Ag-0.5Cu-0.06Ni-0.01Ge solder joints in ball grid array (BGA) packages with Ag/Cu pads. Because the immersion Ag thin film on the Cu pad dissolves rapidly into liquid solder at the onset of the reflow process, it is between Sn-Ag-Cu solders and Cu pads that the interfacial reactions take place, which is similar to the prior cases investigated by Chuang and Lin.[11]

It is well known that the soldering reaction between eutectic Sn-3.5Ag alloy and Cu substrate results in the formation of Cu_6Sn_5 and Cu_3Sn intermetallic compounds at the interface. Accompanying the intermetallic growth, some of the Cu substrate dissolves into the solder matrix. Schaeffer et al. showed that the growth kinetics of interfacial intermetallics was influenced by the amount of the dissolved Cu.[14] Chada et al. further indicated that the rate of Cu dissolution could be described by a Nernst-Brunner equation.[15] The dissolved Cu also caused the formation of Cu_6Sn_5 intermetallics in the Sn-3.5Ag solder matrix, which could be suppressed by increasing the cooling rate.[16] Anderson et al. revealed that the rapidly solidified Sn-3.6Ag-1.0Cu/Cu solder joints possessed a cellular/dendritic microstructure decorated with fine intermetallic phases of Cu_6Sn_5 and Ag_3Sn.[5] The addition of the Co element

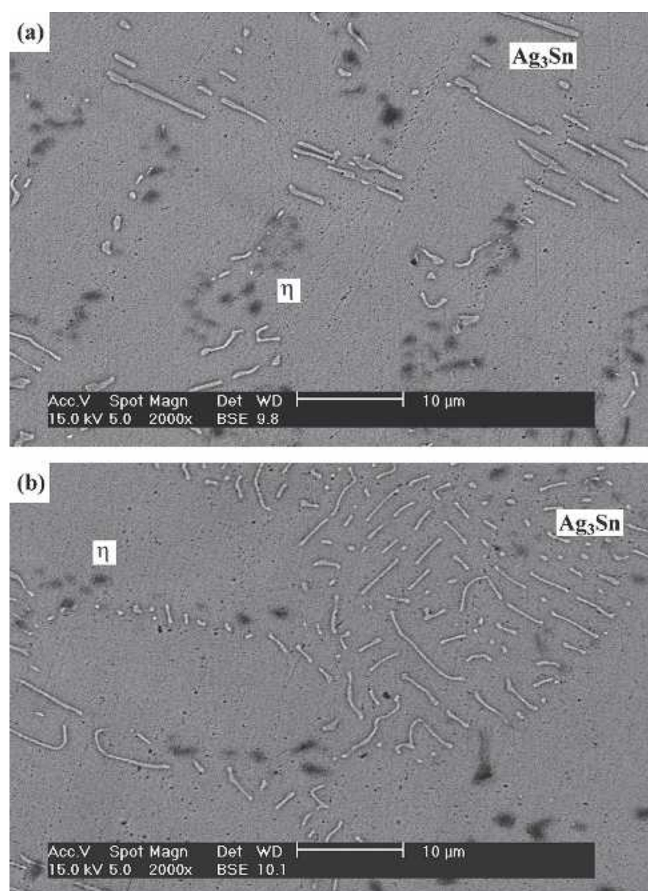

Fig. 2. Microstructure of Sn-Ag-Cu solder balls before reflow: (a) Sn2Ag0.5Cu; (b) Sn3Ag0.5Cu0.06Ni0.01Ge.

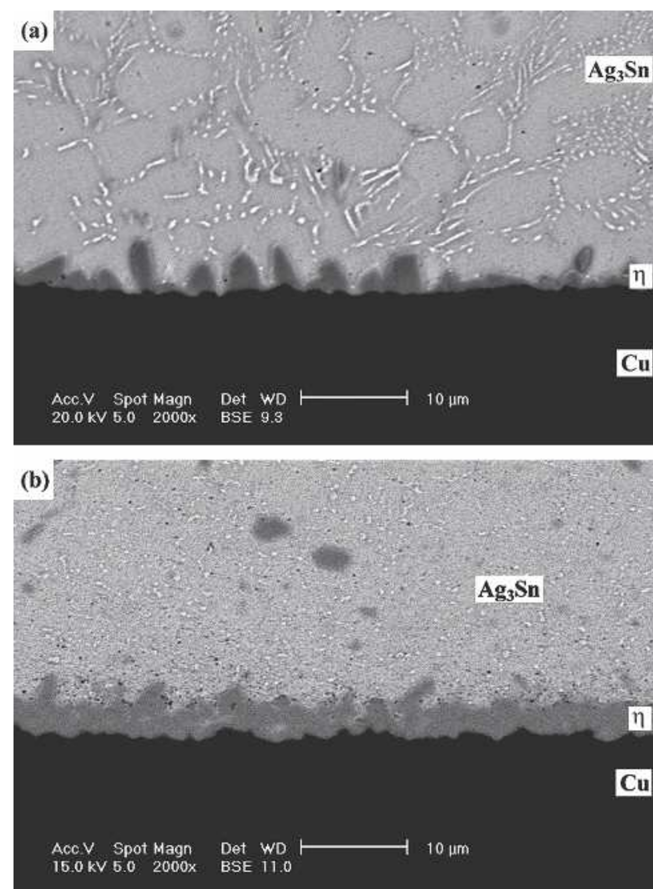

Fig. 3. Morphology of intermetallic compounds formed at the interfaces of the as-reflowed solder joints: (a) Sn3Ag0.5Cu; (b) Sn3Ag0.5Cu0.06Ni0.01Ge.

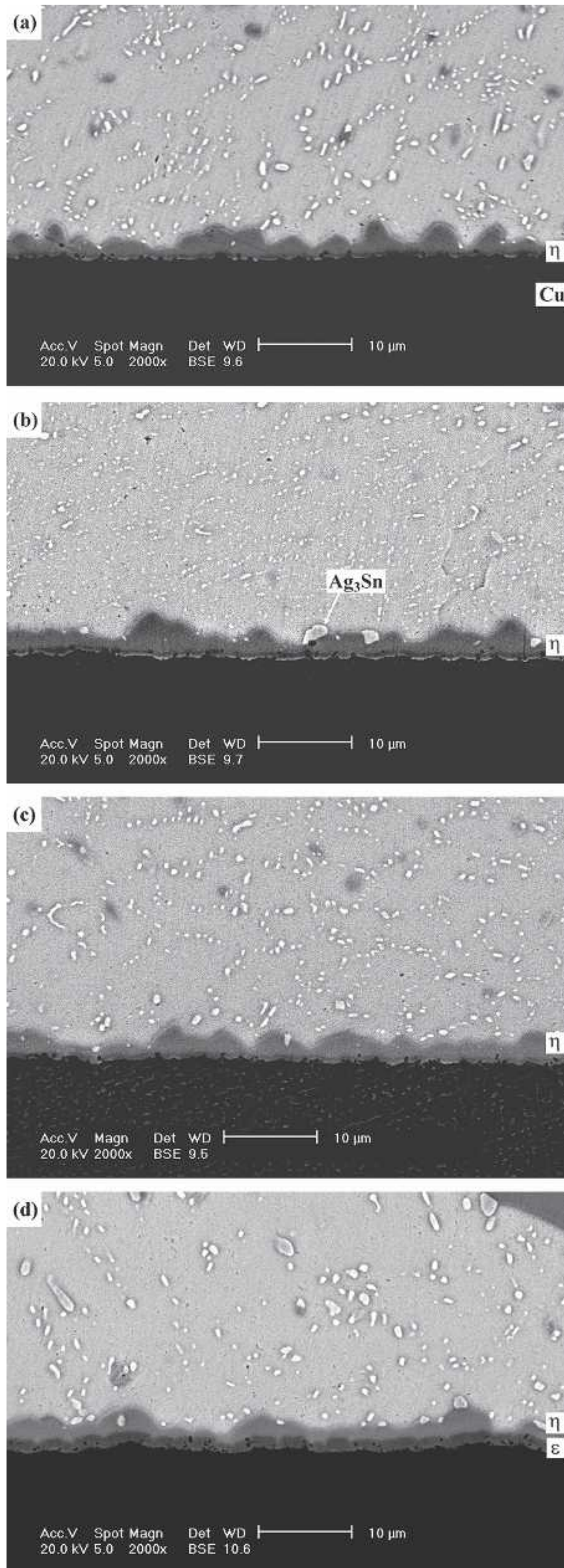

Fig. 4. Morphology of intermetallic compounds formed at the interfaces of the Sn3Ag0.5Cu solder BGA packages with an immersion Ag surface finish after aging at 100°C for various times: (a) 100, (b) 300, (c) 700, and (d) 1000 hr.

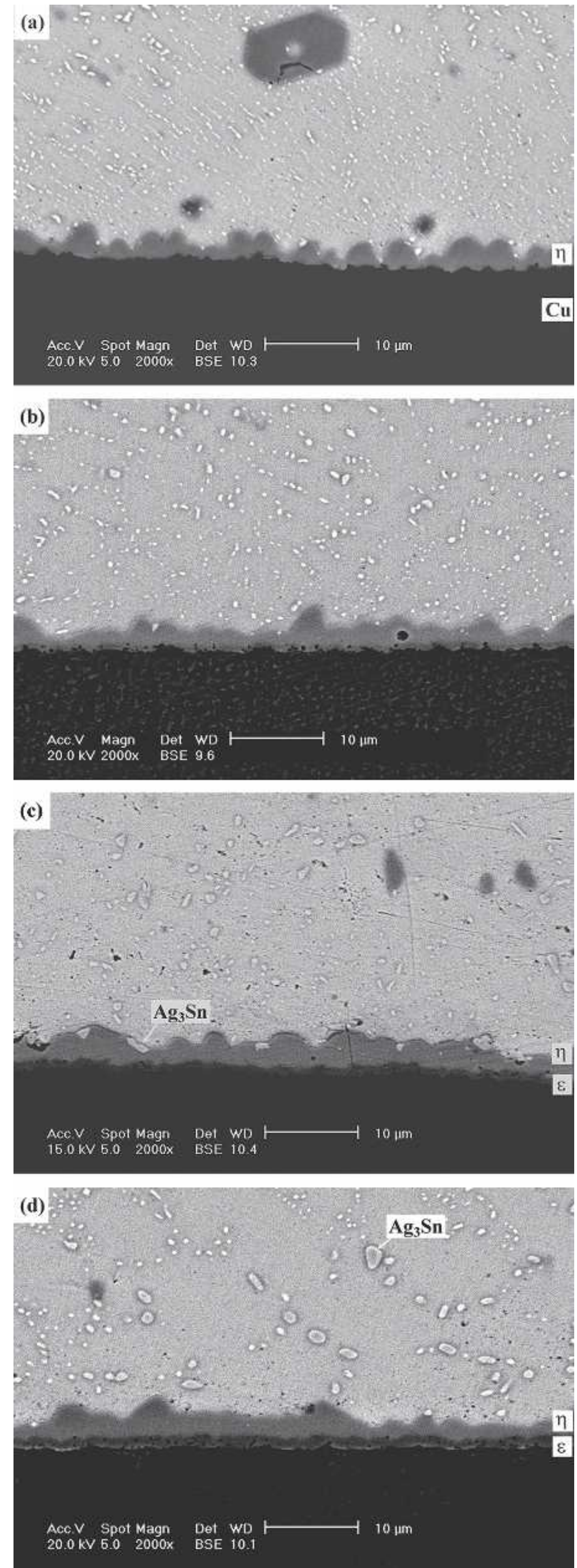

Fig. 5. Morphology of intermetallic compounds formed at the interfaces of the Sn3Ag0.5Cu solder BGA packages with an immersion Ag surface finish after aging at 125°C for various times: (a) 100, (b) 300, (c) 700, and (d) 1000 hr.

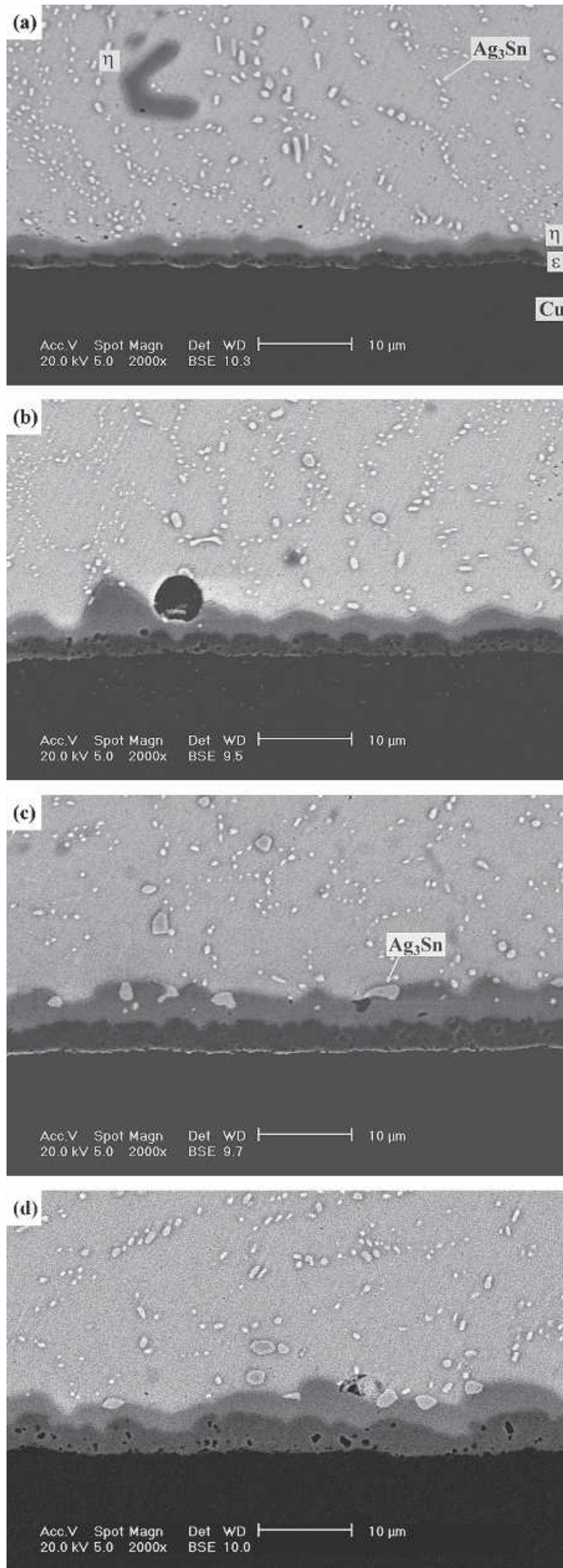

Fig. 6. Morphology of intermetallic compounds formed at the interfaces of the Sn3Ag0.5Cu solder BGA packages with an immersion Ag surface finish after aging at 150°C for various times: (a) 100, (b) 300, (c) 700, and (d) 1000 hr.

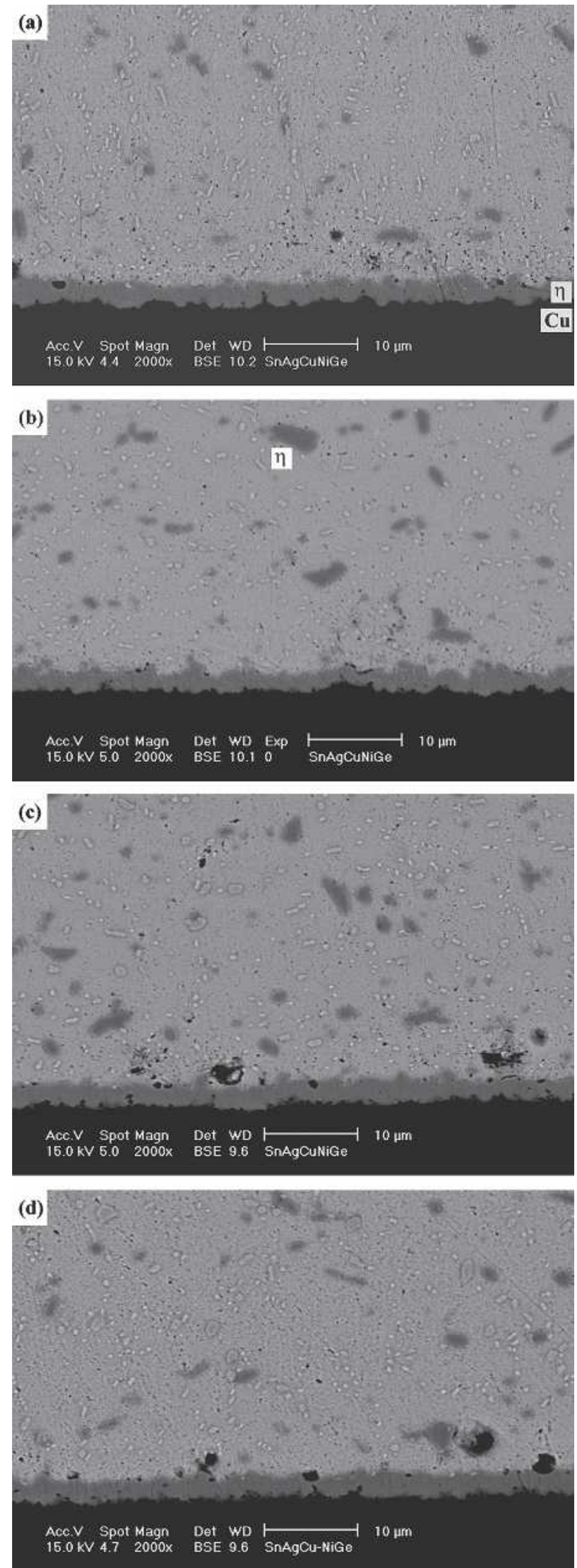

Fig. 7. Morphology of intermetallic compounds formed at the interfaces of the Sn3Ag0.5Cu0.06Ni0.01Ge solder BGA packages with an immersion Ag surface finish after aging at 100°C for various times: (a) 100, (b) 300, (c) 700, and (d) 1000 hr.

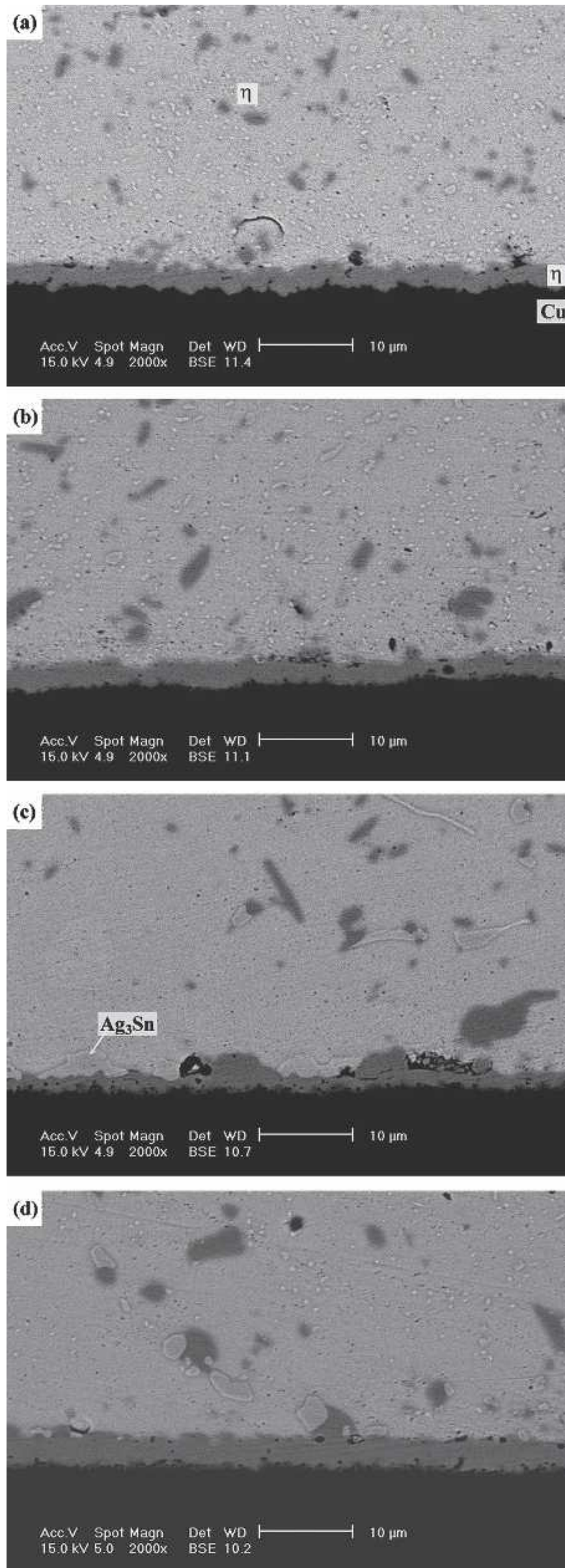

Fig. 8. Morphology of intermetallic compounds formed at the interfaces of the Sn3Ag0.5Cu0.06Ni0.01Ge solder BGA packages with an immersion Ag surface finish after aging at 125°C for various times: (a) 100, (b) 300, (c) 700, and (d) 1000 hr.

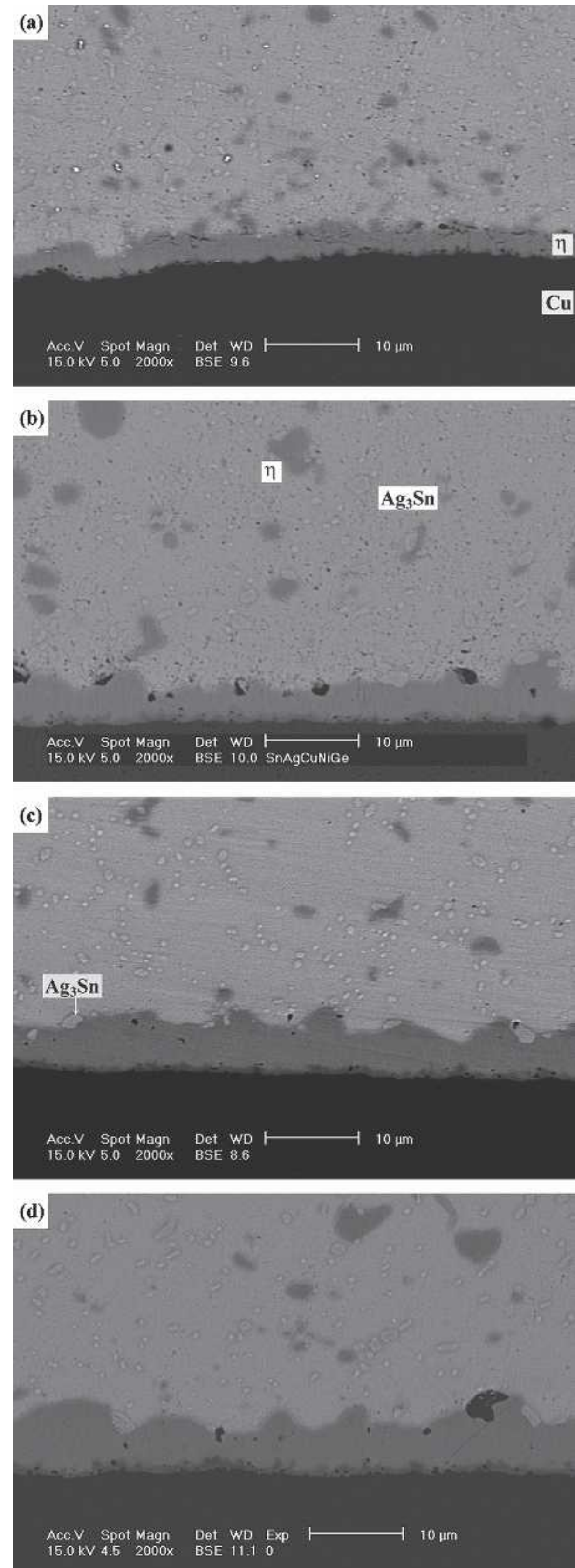

Fig. 9. Morphology of intermetallic compounds formed at the interfaces of the Sn3Ag0.5Cu0.06Ni0.01Ge solder BGA packages with an immersion Ag surface finish after aging at 150°C for various times: (a) 100, (b) 300, (c) 700, and (d) 1000 hr.

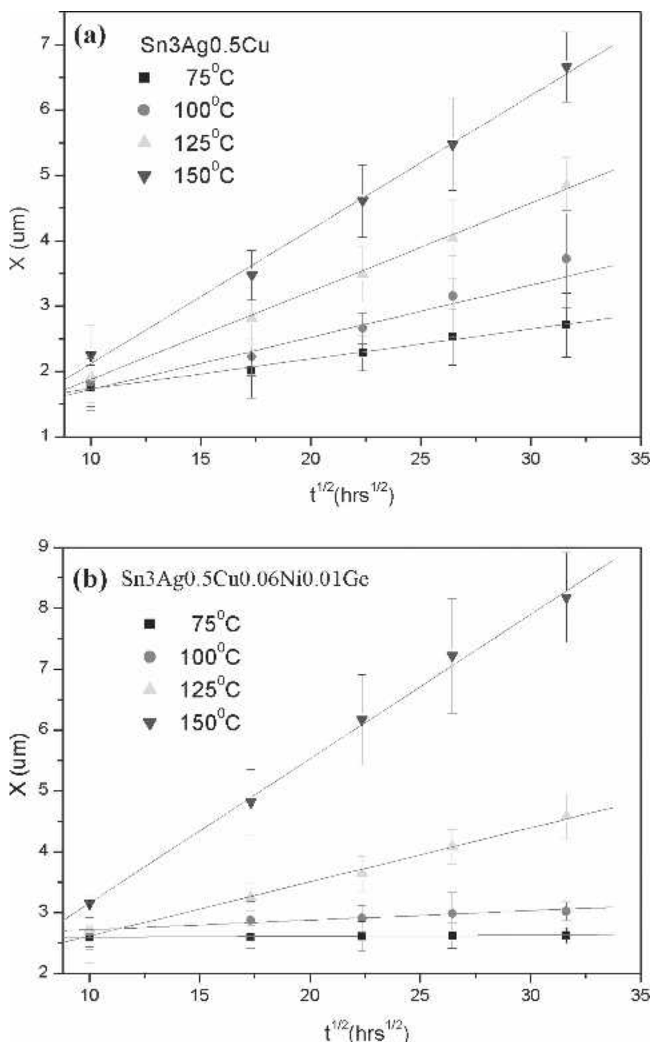

Fig. 10. Growth thickness (X) of η-$(Cu_{0.9}Ni_{0.1})_6Sn_5$ intermetallic compounds during the aging of (a) Sn3Ag0.5Cu and (b) Sn3Ag0.5Cu0.06Ni0.01Ge solder BGA packages as a function of the square root of time ($t^{1/2}$).

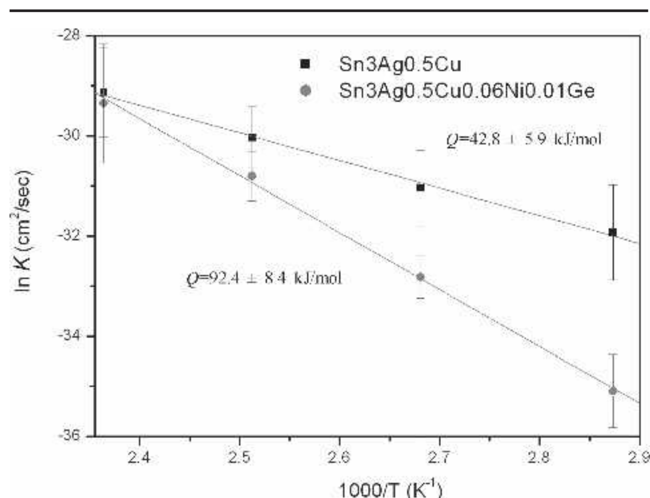

Fig. 11. Arrhenius plots of the reaction constants (K) for growth kinetics of η-$(Cu_{0.9}Ni_{0.1})_6Sn_5$ interfacial intermetallics in the Sn3Ag0.5Cu and Sn3Ag0.5Cu0.06Ni0.01Ge BGA packages.

into Sn-3.6Ag-1.0Cu solder was also reported by Anderson et al. to show a beneficial effect on its shear strength induced by refining the joint microstructure.

EXPERIMENTAL PROCEDURES

The ball-grid array (BGA) package used in this study had 49 Cu pads on a FR-4 substrate, and the surfaces of the Cu pads were immersion-plated with 0.2-μm thick Ag. Sn3Ag0.5Cu and Sn3Ag0.5Cu0.06Ni0.01Ge (wt.%) solder balls 0.4 mm in diameter were dipped in rosin mildly activated (RMA)-type flux, placed on these Ag/Cu pads, and then reflowed in a hot-air furnace. The temperature profile for the reflow of both solder BGA packages is shown in Fig. 1, where the soaking and peak temperatures were fixed at 190 and 240°C, respectively. A certain number of reflowed specimens were further aged at 100, 125, and 150°C for various times ranging from 100 to 1000 hr.

For metallographic observation via scanning electron microscopy (SEM), the reflowed and aged BGA packages were cross-sectioned through a row of solder balls, ground with 2000-grit SiC paper, and then

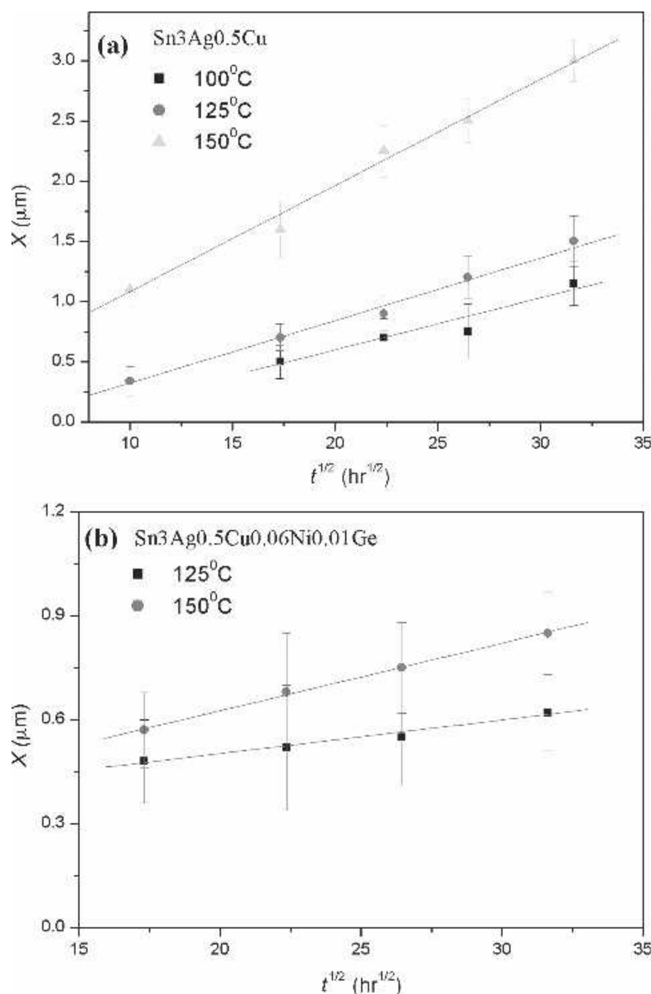

Fig. 12. Growth thickness (X) of ε-Cu_3Sn intermetallic compounds during the aging of (a) Sn3Ag0.5Cu and (b) Sn3Ag0.5Cu0.06Ni0.01Ge solder BGA packages as a function of the square root of time ($t^{1/2}$).

Table I. Ball Shear Strengths (N) of Sn3Ag0.5Cu and Sn3Ag0.5Cu0.06Ni0.10Ge BGA Packages with Ag/Cu Pads After Reflow and Aging Under Various Conditions

	Sn3Ag0.5Cu				Sn3Ag0.5Cu0.06Ni0.01Ge			
Aging Time (hr)	**75°C**	**100°C**	**125°C**	**150°C**	**75°C**	**100°C**	**125°C**	**150°C**
As reflowed	6.61	6.61	6.61	6.61	6.56	6.56	6.56	6.56
100	6.06	5.63	5.77	5.67	6.21	6.11	5.96	5.99
300	5.98	5.53	5.36	5.26	6.11	5.84	5.64	5.54
500	5.79	5.37	4.89	4.73	6.05	5.74	5.15	5.01
700	5.77	5.37	4.85	4.73	6.05	5.65	5.05	4.96
1000	5.62	5.28	4.75	4.51	6.04	5.42	4.84	4.77

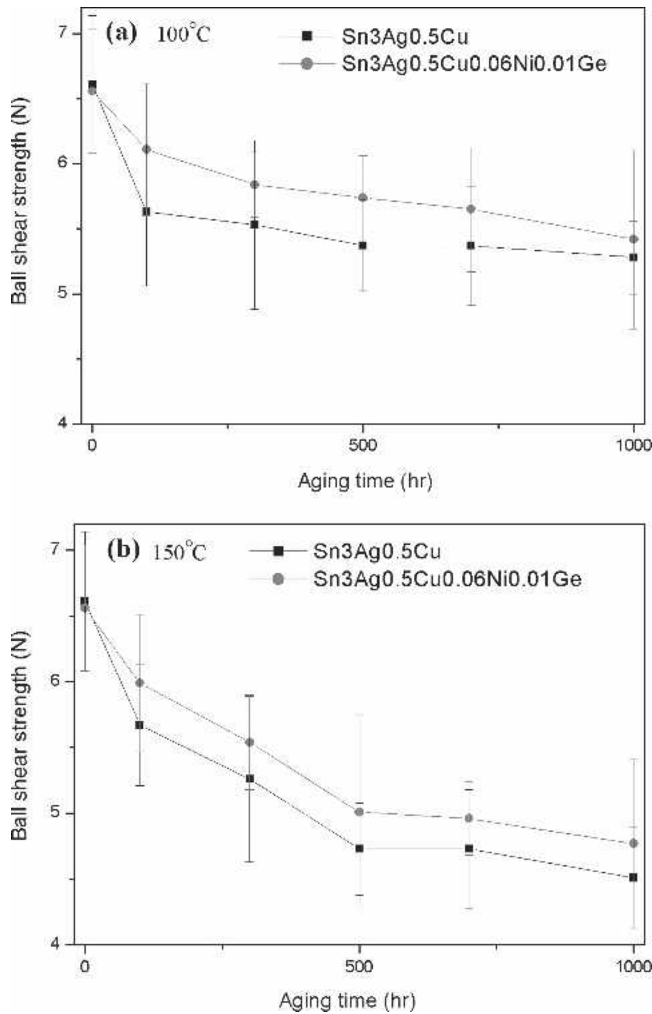

Fig. 13. Ball shear strengths of the solder joints in Sn3Ag0.5Cu and Sn3Ag0.5Cu0.06Ni0.01Ge solder BGA packages with Ag/Cu pads after aging at (a) 100°C and (b) 150°C for various times.

polished with 0.3-μm Al_2O_3 powder. The chemical compositions of interfacial intermetallic compounds were analyzed with an energy-dispersive x-ray spectrometer (EDX) in the SEM. For kinetic analysis, the maximum growth distances of convex scallops for each intermetallic layer were measured. The average value of a minimum of 30 measurements for each soldering condition (per reaction temperature and time) was determined to signify the intermetallic thickness (*X*).

The bonding strengths of the solder joints in the BGA packages were measured via ball shear tests. The measurements were taken at a shear rate of 0.1 mm/sec and a shear height of 80 μm (about ¼ of the reflowed ball height). The fractography of the solder joints after ball shear testing was observed in the SEM.

RESULTS AND DISCUSSION

The microstructures of Sn3Ag0.5Cu and Sn3Ag0.5Cu0.06Ni0.01Ge solder balls before reflow are similar, containing needle-shaped Ag_3Sn and cluster-shaped Cu_6Sn_5 precipitates (Fig. 2). However, intermetallic compounds showing distinct morphological differences appear at the interfaces of the Sn3Ag0.5Cu and Sn3Ag0.5Cu0.06Ni0.01Ge solder joints after reflow. In the case of the Sn3Ag0.5Cu BGA package, scallop-shaped η-Cu_6Sn_5 intermetallics are formed at the solder/pad interface, as shown in Fig. 3a. On the other hand, a continuous planar intermetallic layer with the composition of $(Cu_{0.9}Ni_{0.1})_6Sn_5$ is found at the interface of the Sn3Ag0.5 Cu0.06Ni0.01Ge solder joint (Fig. 3b). In both cases, the immersion Ag thin film on the Ag/Cu pads has dissolved into the solder matrix. Further aging of the Sn3Ag0.5Cu BGA specimen at 100°C results in the growth of η-Cu_6Sn_5 intermetallic scallops, as shown in Fig. 4. It can also be observed in Fig. 4 that the needle-shaped Ag_3Sn precipitates have resolidified into fine particles. When the aging temperature is increased to 125°C, the scallop-shaped Cu_6Sn_5 intermetallic layer becomes more continuous (Fig. 5). When the specimen is aged at 125°C for durations of more than 300 hr, a thin ε-Cu_3Sn intermetallic layer is formed at the interface between the η-Cu_6Sn_5 intermetallic scallops and the Cu pad. Figure 5 also reveals a large number of voids present in the newly appeared ε-Cu_3Sn intermetallic layer. In addition, those Ag_3Sn precipitates in the solder matrix coarsen with the increase of the aging time, as shown in Figs. 4d and 5d. The formation of ε-Cu_3Sn interfacial intermetallics becomes much more conspicuous (Fig. 6) as the Sn3Ag0.5Cu BGA package is aged at 150°C. It is also shown in Fig. 6 that the interior of the ε-Cu_3Sn intermetallic layer is filled with voids. Liu et al.[17] and Vianco et al.[18] have already reported the appearance of Kirkendall voids in Cu_3Sn intermetallics. Because the diffusion coefficient of Cu in

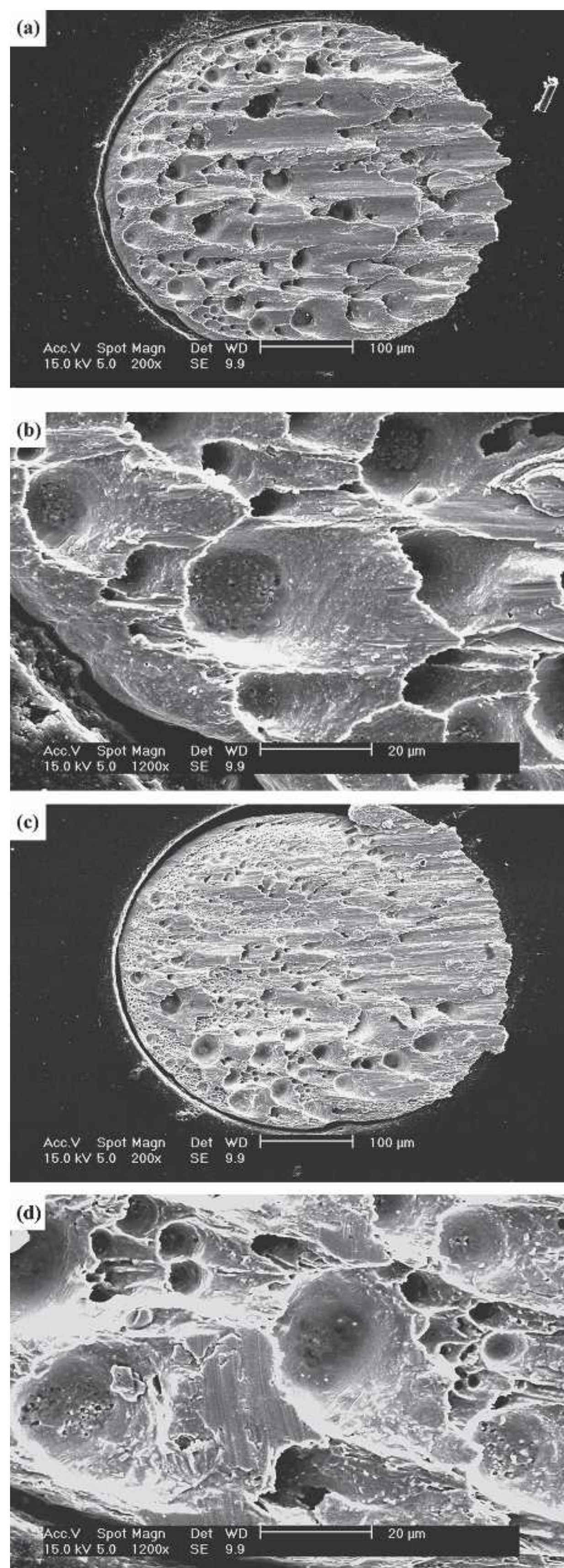

Fig. 14. Typical fractography of the solder joints in BGA packages after ball shear tests: (a, b) Sn3Ag0.5Cu; (c, d) Sn3Ag0.5Cu0.06Ni0.01Ge.

ε-Cu_3Sn intermetallics is greater than that of Sn, as explained by Prinz and Wever,[19] the unbalanced interdiffusion causes Kirkendall voids to build up in the layer of Cu_3Sn intermetallic compounds.

Figures 7–9 show the morphology of the intermetallic compounds formed after the aging of the Sn3Ag0.5Cu0.06Ni0.01Ge BGA packages at various temperatures. The results indicate that the continuous η-$(Cu_{0.9}Ni_{0.1})_6Sn_5$ intermetallic planar layer grows with the aging temperature and time. However, in contrast to what happens in the aging of the Sn3Ag0.5Cu specimens, the formation of the ε-Cu_3Sn intermetallic phase is obviously inhibited. Even after aging at 150°C for prolonged times of 700 and 1000 hr, what can be observed (Fig. 9c and d) is simply a very thin layer of ε-Cu_3Sn with Kirkendall voids. In addition, comparing Figs. 4d and 7d, it is evidenced that the Ag_3Sn precipitates in the Sn3Ag0.5Cu0.06Ni0.01Ge solder matrix coarsened more slowly than those in the Sn3Ag0.5Cu specimens after the aging treatments.

The growth thicknesses of η-$(Cu_{0.9}Ni_{0.1})_6Sn_5$ interfacial intermetallics formed during the aging of Sn3Ag0.5Cu and Sn3Ag0.5Cu0.06Ni0.01Ge solder BGA packages are plotted in Fig. 10 vs. the square root of time. The linear relation of each curve implies that the reaction is diffusion-controlled. Figure 10 also indicates that the Sn3Ag0.5Cu0.06Nu0.01Ge BGA packages possess thicker η-intermetallic compounds at the early stage of aging. However, as the aging time increases, the growth rate of η-intermetallics for the Sn3Ag0.5Cu packages become higher than that for the Sn3Ag0.5Cu0.06Ni0.01Ge packages. Figure 11 shows the calculation from the Arrhenius plots for reaction constants ($K = \Delta x^2/t$), and the activation energies for the growth kinetics of η-intermetallics are thus determined to be 42.8 ± 5.9 and 92.4 ± 8.4 kJ/mol for the Sn3Ag0.5Cu and Sn3Ag0.5Cu0.06Ni0.01Ge packages, respectively. The activation energy for the Sn3Ag0.5Cu0.06Ni0.01Ge BGA packages is higher, which implies that the growth reaction of η-intermetallics in this case is much more sensitive to the aging temperature. The growth thicknesses of ε-Cu_3Sn interfacial intermetallics in both solder BGA packages under various aging conditions also exhibited parabolic kinetics (diffusion-controlled), as shown in Fig. 12. However, the ε-Cu_3Sn intermetallics in the Sn3Ag0.5Cu0.06Ni0.01Ge packages grow much more slowly than those in the Sn3Ag0.5Cu specimens.

Ball shear strengths of both BGA packages after reflow and aging under various conditions are listed in Table I and plotted in Fig. 13. The results show that the reflowed Sn3Ag0.5Cu and Sn3Ag0.5Cu0.06Ni0.01Ge BGA packages with the immersion Ag surface finish possess similar bonding strengths of 6.61 and 6.56 N, respectively. After aging at 100 and 150°C, the ball shear strengths of both types of BGA packages decrease gradually with increased aging time. The bonding strengths of the

Sn3Ag0.5Cu packages are slightly lower than those of the Sn3Ag0.5Cu0.06Ni0.01Ge specimens, which can be attributed to the higher tendency of Ag_3Sn precipitates to coarsen. The fractography of the solder joints in both packages after the ball shear tests reveals the ductile fracture characteristic across the solder matrix (Fig. 14). However, fractographic analysis of the fractured Sn3Ag0.5Cu specimens confirms that the dimples are of a greater size and number than those in the Sn3Ag0.5Cu0.06Ni0.01Ge specimens. The higher tendency of Ag_3Sn to coarsen should also be reflected in this phenomenon.

CONCLUSIONS

Before reflow, Sn3Ag0.5Cu and Sn3Ag0.5Cu0.06Ni0.01Ge solders possess similar microstructures. After reflow, scallop-shaped η-Cu_6Sn_5 and continuous planar η-$(Cu_{0.9}Ni_{0.1})_6Sn_5$ intermetallics, two types of intermetallic compounds with different morphological characterizations, appear at the interfaces of the Sn3Ag0.5Cu and Sn3Ag0.5Cu0.06Ni0.01Ge solder joints, respectively. With increases in aging time and temperature, the η-Cu_6Sn_5 intermetallic scallops in the Sn3Ag0.5Cu specimens become continuous, and an additional ε-Cu_3Sn intermetallic layer is formed at the interfaces between the η-Cu_6Sn_5 intermetallics and the Cu pads. A large number of Kirkendall voids can be observed to exist in the ε-Cu_3Sn intermetallic layer. For the Sn3Ag0.5Cu0.06Ni0.01Ge packages, the formation of the ε-Cu_3Sn intermetallic phase accompanied with Kirkendall voids is inhibited. The growth of η-intermetallics is diffusion-controlled in both the Sn3Ag0.5Cu and Sn3Ag0.5Cu0.06Ni0.01Ge packages, showing activation energies (Q) of 42.8 ± 5.9 and 92.4 ± 8.4 kJ/mol, respectively. The reflowed Sn3Ag0.5Cu and Sn3Ag0.5Cu0.06Ni0.01Ge BGA packages with the immersion Ag surface finish possess similar strengths of 6.61 and 6.56 N, respectively. After aging at 75 and 125°C, the bonding strengths of both packages decrease gradually with increased aging time, which is attributed to the coarsening of Ag_3Sn precipitates in the solder matrix.

ACKNOWLEDGEMENT

The authors express sincere thanks to National Science Council, Taiwan, for the sponsorship of this research under grant NSC-93-2216-E002-024.

REFERENCES

1. K. Zeng and K.N. Tu, *Mater. Sci. Eng. R* 38, 55 (2002).
2. B.L. Chen and G.Y. Li, *53rd Electronic Components and Technology Conf.* (Piscataway, NJ: IEEE, 2003), p. 1235.
3. X. Ma, F. Wang, Y. Qian, and F. Yoshida, *Mater. Lett.* 57, 3361 (2003).
4. B.L. Chen and G.Y. Li, *Thin Solid Films* 462–463, 395 (2004).
5. I.E. Anderson, J.C. Foley, B.A. Cook, J. Harringa, R.L. Terpstra, and O. Unal, *J. Electron. Mater.* 30, 1050 (2001).
6. J. Zhao, L. Qi, X.M. Wang, and L. Wang, *J. Alloys Compd.* 375, 196 (2004).
7. K. Habu, N. Takeda, H. Watanabe, H. Ooki, J. Abe, T. Saito, Y. Taniguchi, and K. Takayama, *Proc. Int. Conf. Electron. Environment,* (New York: IEEE, 1999), p. 21.
8. Z.G. Chen, Y.W. Shi, Z.D. Xia, and Y.F. Yan, *J. Electron. Mater.* 31, 1122 (2002).
9. Z. Chen, Y. Shi, and Z. Xia, *J. Electron. Mater.* 33, 964 (2004).
10. M. Yamashita, S. Tada, and K. Shiokawa (Fuzi Electric. Co.), "Solder Alloys," U.S. patent 6,179,935 B1 (2001).
11. C.M. Chuang and K.L. Lin, *J. Electron. Mater.* 32, 1426 (2003).
12. C.M. Chuang, P.C. Shi, and K.L. Lin, *Proc. Int. Conf. Electron. Mater. Packag.* (New York: IEEE, 2002), p. 360.
13. C.M. Chuang, P.C. Shi, and K.L. Lin, *J. Electron. Mater.* 33, 1 (2004).
14. M. Schaeffer, W. Laub, R.A. Fournelle, and J. Liang, *Design and Reliability of Solders and Solder Interconnections*, ed. R.K. Mahidhara et al. (Warrendale, PA: TMS, 1997), p. 247.
15. S. Chada, R.A. Fournelle, W. Laub, and D. Shangguan, *J. Electron. Mater.* 29, 1214 (2000).
16. S. Chada, A. Hermann, W. Laub, R.A. Fournelle, D. Shangguan, and A. Achar, *Soldering Surf. Mount Technol.* 9, 9 (1997).
17. C.Y. Liu, K.N. Tu, T.T. Sheng, C.H. Tung, D.R. Frear, and P. Elenius, *J. Appl. Phys.* 87, 750 (2000).
18. P.T. Vianco, J.A. Rejent, and P.F. Hlava, *J. Electron. Mater.* 33, 991 (2004).
19. N. Prinz and H. Wever, *Phys. Status Solidi A* 61, 505 (1998).